High-Strength Steel Development for Pipelines: A Brazilian Perspective

IVANI DE S. BOTT, LUIS F.G. DE SOUZA, JOSÉ C.G. TEIXEIRA, and PAULO R. RIOS

The production of American Petroleum Institute (API) class steels using the traditional controlled rolling route rather than the process involving accelerated cooling necessitates a careful adjustment of steel composition associated with the optimization of the rolling schedule for the deformation and phase transformation characteristics of these modified alloys. The current work presents a study of two, NbCr and NbCrMo, steel systems. The microstructure obtained is correlated not only with the resulting mechanical properties, but also with the weldability and resistance to damage in the aggressive environments to which the materials are exposed. The evaluation of the steels was undertaken at two stages along the production route, sampling the material as plate and as tubular product, according to the API 5L 2000 standard. Tensile testing, Charpy-V impact testing, and hardness measurements were used to determine the mechanical properties, and microstructural characterization was performed by optical and scanning electron microscopy. The results showed that it was possible to obtain good impact properties, for both steels, in plate and tube formats. The Charpy-V impact energy, measured at −20 °C from 100 to 250 J corresponds to a toughness level above that required by the API 5L 2000 standard, which specifies 68 to 101 J at 0 °C. The yield strength (YS) to ultimate tensile strength (UTS) ratio was determined to be 0.8, the API standard establishing a maximum limit of 0.93. Both of the alloys investigated exhibited a bainitic microstructure and were successfully processed to fabricate tubular products by the "UOE" (bending in "U", closing in "O," and expanding "E") route. With regard to weldability, the two experimental steels exhibited a heat-affected zone (HAZ) for which toughness levels (using the temperature associated with a 100 J impact energy as a base for comparison) were higher than those for both the base metal (BM) and the weld metal (WM) itself. In order to perform the evaluation of the behavior of the steels in an aggressive environment, more specifically their resistance to the deleterious effects of H_2S, slow strain rate tests (SSRTs) were carried out, immersing the samples in a sodium thiosulfate solution during the tests. Though no secondary cracking was observed in the test samples, the ductility levels measured were lower than those for the same materials tested in air. Constant load tests were also conducted according to the standard NACE conditions. Despite the more aggressive nature of the test solution in these cases, no samples of either steel suffered failure.

I. INTRODUCTION

THE significant economic advantages of transporting crude oil and gas by pipeline has led not only to a growing demand for extensive pipeline networks, but also a need to increase the capacity of the existing ones. Such an increase in capacity necessitates the installation of larger diameter pipes and higher operating pressures, and consequently requires the use of thicker walled pipes or higher strength steels.

Increasing the strength of the pipeline material used can permit a significant reduction in wall thickness, thereby resulting in economic benefits due to the reduction in overall weight. Such savings are especially important for pipeline construction in remote locations, where any weight reduction can be critical in reducing basic costs such as those associated with transport and manipulation during construction and welding.

IVANI DE S. BOTT, Associate Professor, is with the DCMM/PUC-Rio, Rio de Janeiro-RJ, 22453-900 Brazil. Contact e-mail: bott@dcmm.puc-rio.br LUIS F.G. DE SOUZA, Adjunct Professor, is with the DEPMC/CEFET-RJ, Rio de Janeiro-RJ, 20271-110 Brazil. JOSÉ C.G. TEIXEIRA, Senior Engineer, is with the PETROBRÁS/CENPES, Rio de Janeiro-RJ, 21949-900 Brazil. PAULO R. RIOS, Professor, is with the UFF/EEIMVR, 420, Volta Redonda-RJ, 27255-125 Brazil.

Manuscript submitted December 22, 2003.

A particularly important advance in the development of pipeline steels occurred in the 1970s with the introduction of thermomechanical processing to substitute for the traditional heat treatment production routes. This was the basis for the manufacture of X-70 steels, which soon became the industry standard for pipeline construction.[1]

The subsequent introduction of accelerated cooling after controlled rolling led to the possibility of producing steels with even higher strength levels.[2] The American Petroleum Institute (API) X-80 steels, though to date used little in Brazil, have been very successfully exploited worldwide in pipeline construction. These steels have been manufactured using a production route, which includes accelerated cooling at cooling rates of 15 to 20 °C/s until reaching a temperature of around 550 °C, after which air cooling is used. In Brazil, the production of API class steels using the traditional controlled rolling route, rather than the process involving accelerated cooling, necessitates a careful adjustment of steel composition associated with the optimization of the rolling schedule for the deformation and phase transformation characteristics of these modified alloys.

This work examines the feasibility of exploiting two steels produced without accelerated cooling in pipeline applications. The microstructure-toughness relationship of the steel as plate, tube, and longitudinal welded joint was evaluated.

The effect of an aggressive environment on the body pipe was also studied.

II. WELDABILITY

The "UOE" (bending in "U", closing in "O," and expanding "E") pipeline fabrication process involves internal and external longitudinal submerged arc welding using the Tandem technique. This process results in high heat input. When applied to high-strength steels, this process can lead to heat-affected zone (HAZ) softening, though not necessarily a reduction in strength of the welded joint.[3]

The weldability, formability, and fracture toughness requirements for typical pipeline steels led to the necessity of maintaining a particularly low volume fraction of nonmetallic inclusions, which should be small and globular, which in turn demands low oxygen and sulfur contents. The established practice of aluminum-based deoxidation procedures removes the majority of the oxygen from the melt in the form of oxides. Some aluminum, however, remains in the steel, and that which is not precipitated as alumina can be exploited as a grain refining agent, when appropriately precipitated as nitride. The precipitates, which effectively influence the final microstructure and properties of these steels, are those formed during the hot working procedures themselves, or on subsequent heat treatment.

For a typical X-80 composition (all compositions in this article are in weight percent) of 0.08 pct C and 1.50 pct Mn, the resulting microstructure of the commercial alloys is one containing ferrite and bainite. In order to increase the strength without significant losses in toughness, a high volume fraction of bainite is desirable. This is obtained, in practice, by increasing the hardenability of the material through the addition of alloying elements such as Mn, Mo, and Ni, which effectively retard the $\gamma \rightarrow \alpha$ transformation.[4]

It should be remembered, however, that the excellent combination of strength and toughness exhibited by modern bainitic-ferritic microalloyed steels produced by controlled rolling can be significantly degraded by the thermal cycles imposed during the fabrication of the final pipeline product and its on-site assembly for service. Welding processes impose such cycles and can lead to local brittle zones in the HAZ, more specifically in the intercritical coarse grain region.[5,6]

In order to counteract such effects, especially the potential loss of toughness of the HAZ, steel producers must take into account the effect of such postrolling processing from the outset, when designing their steel's composition. Small additions of Nb (of the order of 0.02 pct) can effectively reduce the nucleation of ferrite along prior austenite grain boundaries and thereby promote an increase in the volume fraction of bainite.[7] Moreover, the resulting grain refinement can offset the deleterious hardening effects otherwise produced by welding, though the degree to which this will occur in practice depends strongly upon the heat input effectively imposed. The V can also be exploited to good effect, since around 0.05 pct of this element can cause a reduction in the size and overall volume fraction of the martensite-austenite (MA) microconstituent, thereby improving the HAZ toughness.[6]

Improvements in weldability can be achieved by the use of production routes that guarantee low levels of S and P, inclusion control, and reductions in the levels of C, Mn, and Si. Additions of Mn effectively decrease carbon activity in the austenite phase, thereby impeding the bainite transformation and promoting instead the formation of the MA microconstituent.[8]

It has been shown[9,10] that low fracture toughness typically associated with the HAZ is often provoked by certain specific microstructural aspects. In general, in ferritic-pearlitic C-Mn steels, MA occurs due to the intercritical reheating, which is produced by the welding process' thermal cycles. The presence of this microconstituent tends to reduce HAZ toughness. The actual morphology of this constituent, which is usually categorized as either "massive" or "elongated," is also important. It is the elongated form that is principally responsible for the loss in toughness. Other factors must also be considered, one of which is the carbon content of the MA. High-C MA (>0.05 pct) is generally considered to be brittle.[11] Other factors include the volume fraction, size, and distribution of the MA.[12]

III. STRUCTURAL INTEGRITY

The need to guarantee the structural integrity of pipelines is an ever-growing concern, as the results of a catastrophic failure would lead not only to environmental damage, but also potentially injury and loss of life. Such a guarantee of security can only be effectively achieved through an integrated approach, which involves all aspects of quality control during steel production, pipeline fabrication, and assembly as well as during operation and pre-emptive maintenance.

The practical situation is complicated even further by the fact that the oil and gas pipelines, once in service, not only have to routinely withstand high operating pressures, but often also high levels of CO_2, H_2S, and chlorides. The high-strength steels exploited for these applications therefore must be resistant to various aspects of in-service degradation. For example, the nucleation and growth of cracks in carbon and low-alloy steel pipes exposed to fluids containing H_2S can readily lead to catastrophic failure.[13] It can be appreciated, therefore, that the steels to be used in oil and gas pipeline applications must offer an especially wide range of appropriate properties, from high strength and toughness to good weldability and elevated corrosion resistance. The latter should also, in this case, be taken to include resistance to hydrogen-induced damage.

It well known that three conditions are required for stress corrosion cracking (SCC) to occur; the necessary type of aggressive environment, a tensile load, and the susceptibility of the material to such damage. A slow strain rate test (SSRT) has been widely used as a laboratory technique to evaluate the susceptibility of metallic materials to SCC and hydrogen embrittlement. This test has become a popular tool to investigate steels, which are candidates for applications in the oil and gas industries. The test provides rapid testing associated with severe imposed conditions, thereby permitting a wide-ranging evaluation of the material, which includes a significant number of individual tests, within a relatively short period.

The SCC susceptibility is formally quantified according to a rupture/no rupture criterion, using the technique specified in the NACE 0177-96 Standard–Method A (Standard Tensile Test).[14] In this standard, test pieces are subjected to constant, uniaxial, elastic tensile loading for a given time, at ambient temperature and atmospheric pressure, in the

specified aggressive medium. Both methods were used to evaluate the steel susceptibility to cracking.

IV. MATERIAL AND EXPERIMENTAL PROCEDURE

A. *Steel Compositions*

Table I shows the chemical compositions of the two groups of microalloyed steels, an X-80 and an X-70, which were studied. The X-80 steel, subjected to the same processing conditions except for the finishing temperatures, was supplied in the form of 16-mm plates (samples A through L) and also as tubes A, D, G, and J, produced by the UOE process. In the UOE fabrication process, the plate is cold pressed into "U" and to "O" formats sequentially, followed by internal and external welding runs of submerged arc; after this welding stage, the pipe is "expanded" (E). The X-70 was supplied only as a tube. This same table shows the chemical composition of the weld metal (WM) both for the internal and external longitudinal weld of the tube.

In order to more fully evaluate the performance of the two steel systems under study, in addition to the postcontrolled rolling plate, the final tubular product and the HAZ were also investigated.

B. *Microstructure*

The morphology and distribution of the MA microconstituent were analyzed by observing 30 images per sample. These images were captured on the scanning electron microscopy (SEM) at a magnification of 3000 times. A quantitative metallographic examination was performed using a 100-point grid over the captured image. The absolute error was approximately ± 1 vol pct for specimens containing 3 vol pct of MA and ± 1.7 vol pct for specimens containing 5 vol pct of MA. The ferrite mean intercept length grain size, measured by optical microscopy, was equal to 10 μm and was approximately the same for all steels.

C. *Welding Parameters*

The submerged arc welding process (Tandem technique) was used for the internal and external longitudinal welds during tube production. The average parameters, for each of the three wires employed for the industrial scale pipe welding, were current = 750 to 1000 A, voltage = 35 to 40 V, and welding speed = 177 cm/min, which generated a total heat input on the order of 40 kJ/cm.

D. *Hardness Measurements*

All results for the plate were an average of ten measurements along the longitudinal and transverse directions. Results for the HAZ were an average of the measurements taken at 1, 2, and 3 mm from the fusion line through the thickness of the plate.

E. *Sampling Procedure*

Mechanical testing was undertaken according to the API 5L 2000[16] standard, and included tensile testing, Charpy-V impact testing, and Vickers hardness assessments, for the plate material, body pipe, and HAZ, respectively.

Figure 1 is a schematic diagram showing the localization, orientation, and dimensions of the Charpy-V specimens used in this study relative to the body pipe, the WM, and the HAZ regions

Table I. Chemical Composition[15]*

Sample	Plate/Pipe	P_{cm} (Pct)	Elements (Wt Pct)							
			C	Mn	Si	Nb	Ti	Cr	Mo	N
NbCrMo (X-80)	**A**, B, C	0.18	0.07	1.76	0.18	0.071	0.014	0.20	0.16	0.006
	D, E, F	0.15	0.04	1.75	0.17	0.073	0.013	0.21	0.16	0.004
NbCr (X-80)	**G**, H, I	0.16	0.04	1.85	0.18	0.073	0.016	0.32	0.03	0.004
	J, K, L	0.16	0.04	1.86	0.19	0.075	0.017	0.33	0.03	0.005
X-70	—		0.06	1.55	0.18	0.055	0.017	0.02	—	0.0071
WM	**Internal****		0.08	1.97	1.97	0.045	0.010	0.17	0.283	—
	External**		0.07	1.86	1.86	0.044	0.015	0.16	0.300	—

*All steels contain approximately (in wt pct): P-0.02, S-0.005, Al-0.03, Cu-0.01, V-0.005, Ni-0.002, and Ca-0.001.
**The terms "Internal" and "External" refer to the weld made during the tube fabrication, therefore corresponding to the longitudinal submerged arc weld.

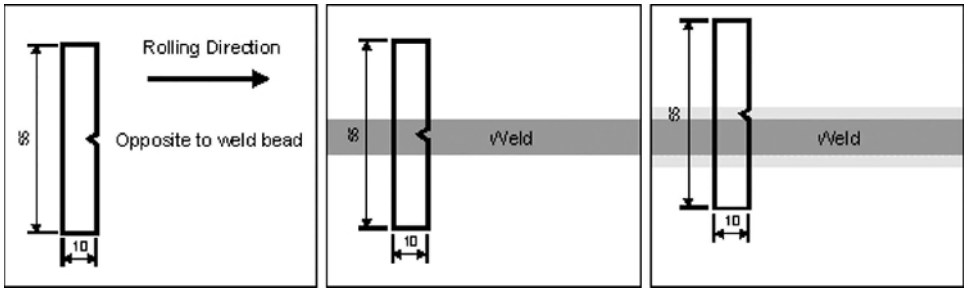

(*a*) (*b*) (*c*)

Fig. 1—Schematic diagram of the sampling procedure for the Charpy-V test pieces: (*a*) body pipe, (*b*) WM, and (*c*) HAZ.

F. *Slow Strain Rate Test*

Table II presents the chemical composition of the test solution used in the SSRT. When the sample is immersed in it, this solution effectively produces H_2S on its surface.

The SSRT at a maximum axial loading of 2000 kgf (1.961×10^4 N) was performed for both X-70 and X-80 steels using cylindrical test pieces as specified in the NACE Standard and under two conditions, in air and in the hydrogen charging solution detailed in Table II.[17]

G. *NACE TM 0177/96 Test—Method A (Standard Tensile Test)*

The NACE TM 0177/96 SCC test[14] was also used in the evaluation of the steels investigated, using the NACE Standard's "solution B," the chemical composition of which is detailed in Table III.

After completing the test, the test piece surfaces, which had been in contact with the test solution, were chemically cleaned according to the ASTM G 1-95 standard, in order to permit a metallographic examination to assess whether superficial cracks had been formed during the test.[17]

Table II. Chemical Composition of the SSRT Solution in Volume Percent[17]

	SSRT Solution Composition		
Component	Sodium Thiosulfate ($Na_2S_2O_3$)	Sodium Chloride (NaCl)	Acetic Acid (CH_3COOH)
Concentration	10^{-3} mol/L	5 pct	0.50 pct

Table III. Chemical Composition of NACE "Solution B" in Volume Percent[17]

	Chemical Composition of the NACE "Solution B"		
Component	Sodium Chloride (NaCl)	Sodium Acetate (CH_3COONa)	Glacial Acetic Acid (CH_3COOH)
Concentration	5 pct	0.4 pct	0.23 pct

V. RESULTS

A. *Microstructure*

Figure 2 shows typical scanning micrographs of the (a) and (b) plate, (c) and (d) HAZ, and (e) and (f) WM. The plate exhibited a ferritic microstructure with martensite-austenite (MA) microconstituent. It can be observed by comparing images 2a and 2b with 2c and 2d that the morphology of the MA microconstituent changed for the HAZ. Table IV shows the result of metallographic examination for the MA microconstituent volume fraction present in the plate and HAZ. The cooling rates experienced by the HAZ produced an increase of the MA microconstituent, but its morphology has been modified (Figures 2(c) and (d)). The corresponding size and area fraction of the MA microconstituent present in the HAZ did not adversely affect its toughness.

B. *Plate Weldability*

The parameter that has been most used in practice to measure steel weldability is the carbon equivalent (CE) formula, where good weldability is in general obtained by maintaining a low CE. This method of evaluation is based upon the empirically identified tendencies in the variation of the M_s temperature as a function of the alloying elements present in the steel.[19]

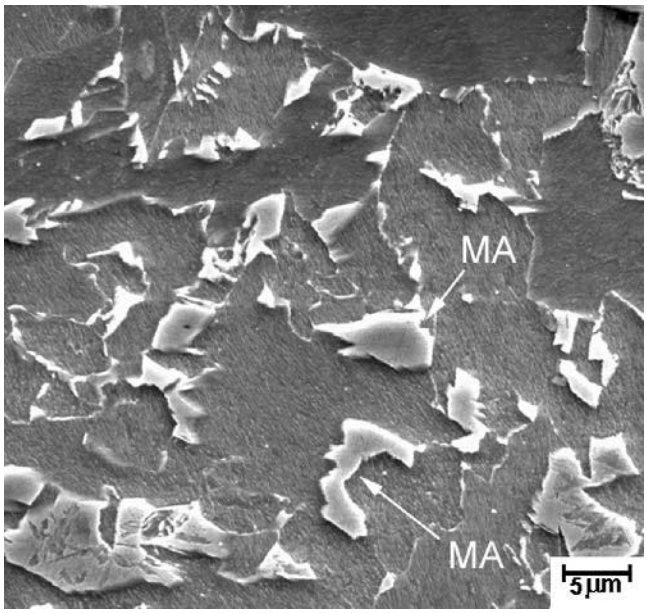

(*a*)

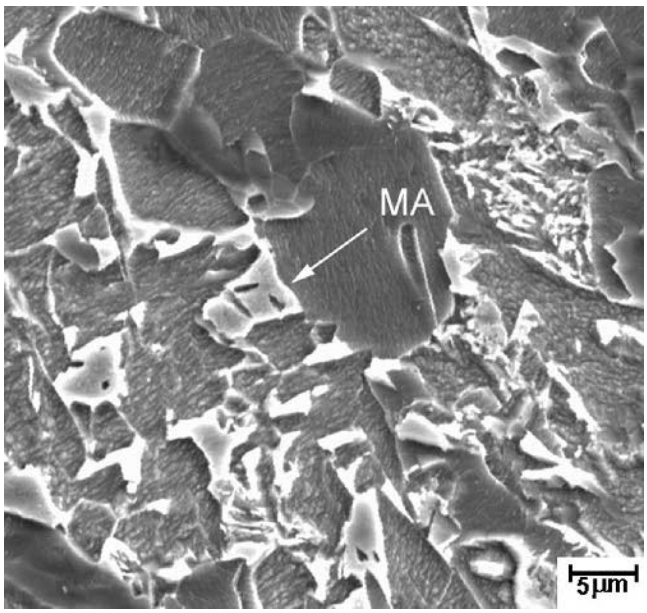

(*b*)

Fig. 2—Typical ferritic microstructure with MA microconstituent, as revealed by scanning electron microscopy of samples of the two systems studied, (*a*) NbCrMo and (*b*) NbCr, corresponding to the steel plates A and G, respectively. (*c*) and (*d*) The HAZ of the longitudinal weld of the tubes originated from plates A and G. (*e*) and (*f*) The WM microstructure of these welds. All samples were etched in 2 pct natal.[15,18]

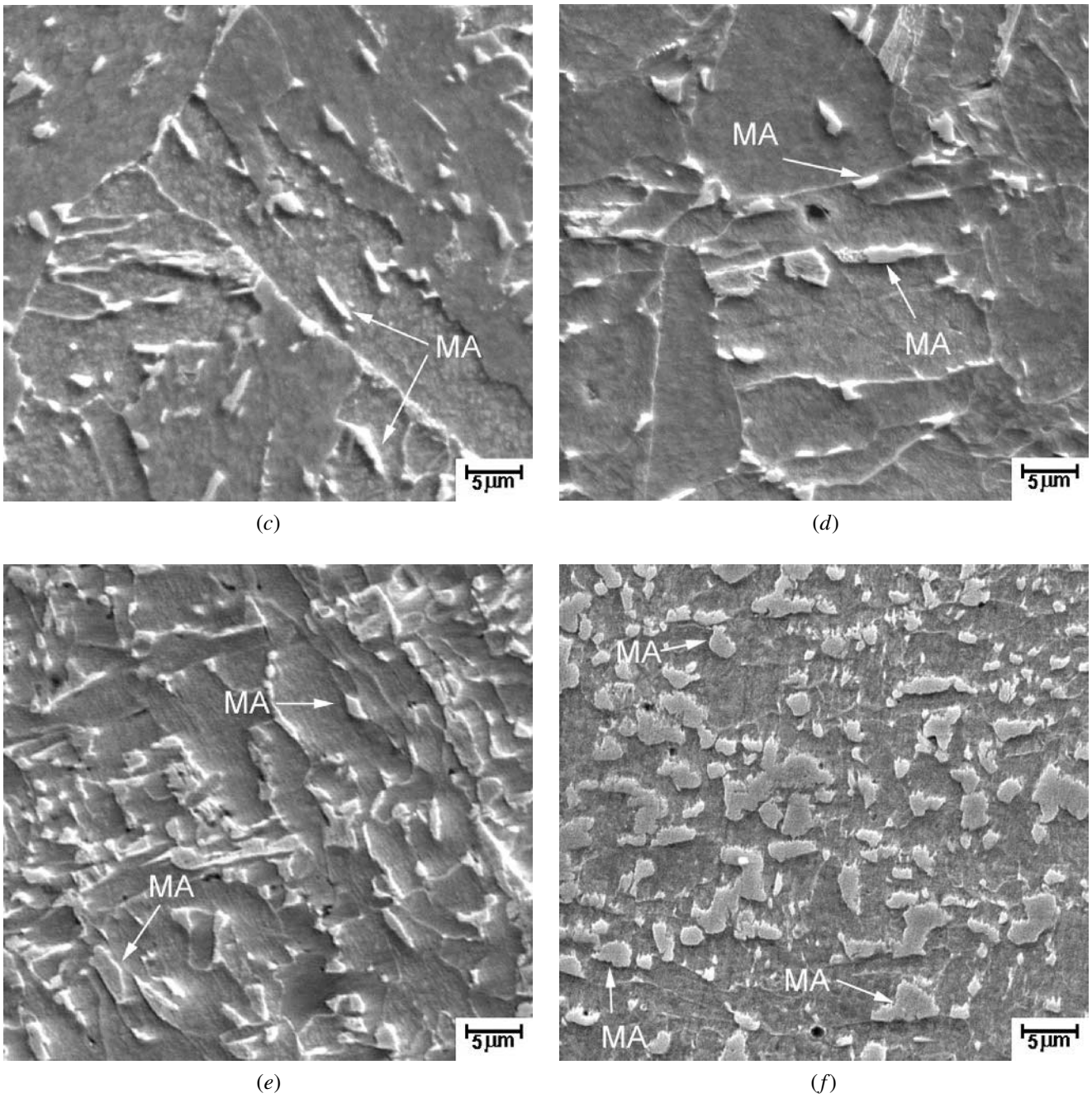

Fig. 2—(Continued). Typical ferritic microstructure with MA microconstituent, as revealed by scanning electron microscopy of samples of the two systems studied, (*a*) NbCrMo and (*b*) NbCr, corresponding to the steel plates A and G, respectively. (*c*) and (*d*) The HAZ of the longitudinal weld of the tubes originated from plates A and G. (*e*) and (*f*) The WM microstructure of these welds. All samples were etched in 2 pct natal.[15,18]

Table IV. MA Microconstituent Volume Fraction Present in the Plate and HAZ[15,18]

System		MA Volume Fraction (Pct)	
		Plate	HAZ
NbCrMo	A	5.1	8.3
	D	5.2	7.3
NbCr	G	3.4	5.3
	J	2.6	7.2

According to the API 5L 2000 standard, the choice of equation to be used in determining the CE of X-80 steels will depend on the C content itself. For alloys with C contents equal to, or below, 0.12 pct, the CE (P_{cm}), or Ito and Bessyo formula should be used (Eq. [1]),[20] for which the maximum permitted CE (P_{cm}) value is 0.25 pct. For steels of higher C contents, the IIW formula should be used.[20]

$$\mathrm{CE}\,(P_{cm}) = \mathrm{C} + \frac{\mathrm{Si}}{30} + \frac{\mathrm{Mn}}{20} + \frac{\mathrm{Cu}}{20} + \frac{\mathrm{Ni}}{60} + \frac{\mathrm{Cr}}{20} + \frac{\mathrm{Mo}}{15} + \frac{\mathrm{V}}{10} + 5\mathrm{B} \qquad [1]$$

In the two steels, NbCr and NbCrMo, under study, for which the C content was between 0.04 and 0.07 pct, the CE values, determined according to the API 5L standard, were as shown in Table I.

In this study, it was observed that the MA volume fraction increased with increasing CE (P_{cm}), for the same level of carbon, 0.04 pct; the NbCrMo steel exhibited a slightly lower P_{cm} than the NbCr steel. Naturally, the most significant increase in P_{cm} was caused by the increase in the level of carbon itself and, at a C level of 0.07 pct, the NbCrMo steel exhibited a P_{cm} of 0.18 pct.

VI. MECHANICAL PROPERTIES

A. *Plate Tensile Strength*

An increase in strength was observed after forming. The resulting yield strength (YS) to ultimate tensile strength (UTS) ratio was below 0.93 (as shown in Figure 3), the maximum permitted by the API 5L Standard.

B. *Plate Toughness*

As shown in Figure 4, the temperature associated with the 100 J absorbed energy level in the impact tests was seen to decrease with decreasing MA volume fractions for both steels investigated

C. *Welded Joint Hardness*

The different regions (base metal (BM), HAZ, and WM) of the submerged arc longitudinal welds were compared with the plate and body pipe, thereby quantifying the microstructural evolution and variations in mechanical properties of the steels throughout not only the industrial-scale production, but also pipeline fabrication routines.

Figure 5 shows the evolution of hardness for the steels under investigation, from the as-rolled plate to the tubular product and in the WM and HAZ (assessed by Vickers microhardness measurements, performed using a load of 100 gf). It can be seen that the HAZ exhibited the lowest hardness and the WM the highest. There was no significant change from plate to tube.

D. *Welded Joint Tensile Strength*

It is known that the thermal cycles associated with the industrial welding process used in pipeline fabrication and construction can lead to localized increases in hardness in the HAZ[21] and a reduction in the YS. No such increase of hardness was observed (Figure 5) or reduction of the UTS (Figure 6(a)) for the steels and conditions studied in the current work.

E. *Welded Joint Toughness*

Figure 7 shows the Charpy-V impact tests for the welded joint considering the BM, HAZ, and WM.

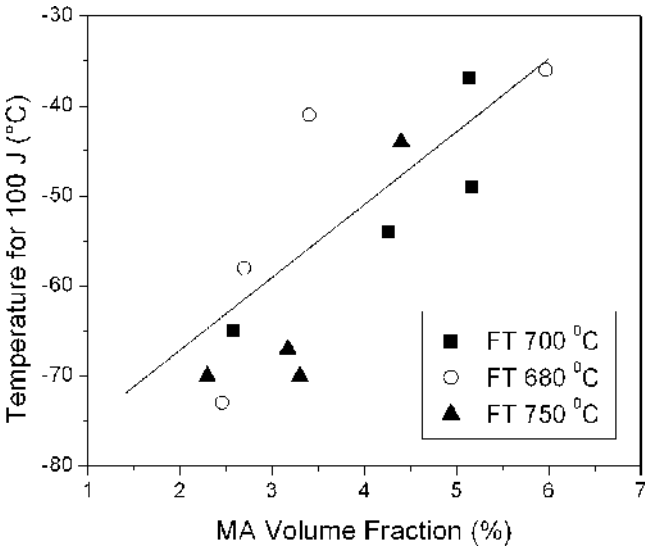

Fig. 4—Relationship between the MA volume fraction and the 100 J absorbed energy level determined by impact testing, as a function of the finishing temperature.[15,18]

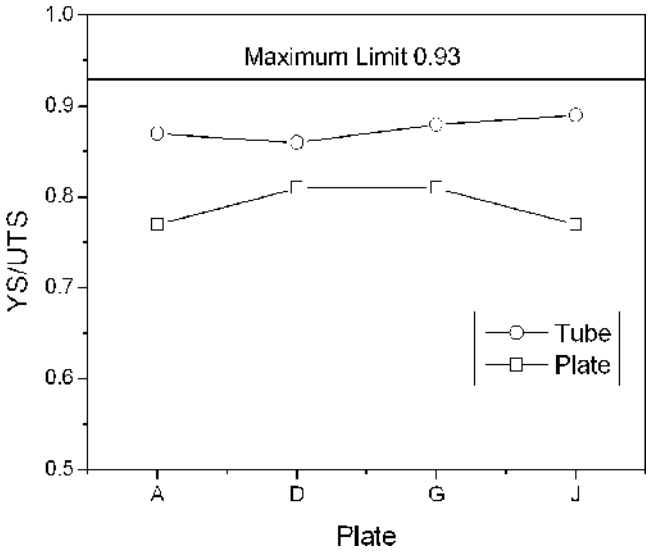

Fig. 3—YS:UTS ratio for the plate and tube.[15,18]

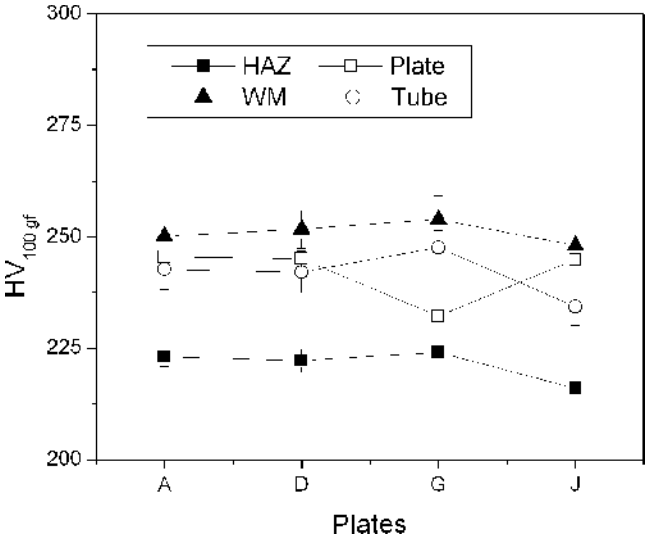

Fig. 5—Vickers microhardness results (100 gf) at several stages during processing and for the weld.

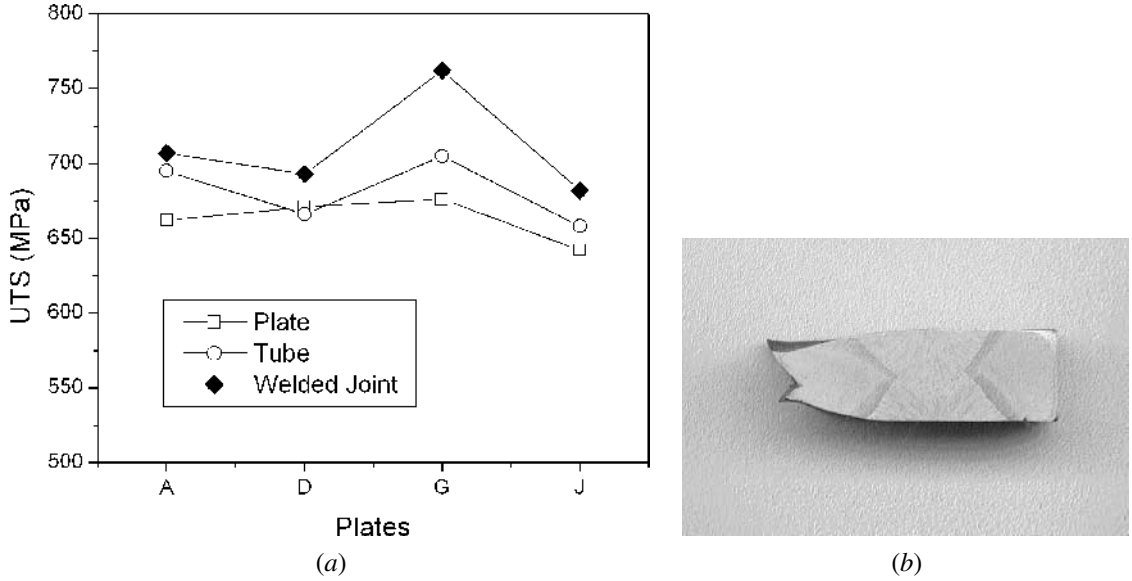

Fig. 6—(*a*) Comparison of YS and UTS for the steels under study. (*b*) Typical appearance of sample rupture in the tensile test, for the steels under study.

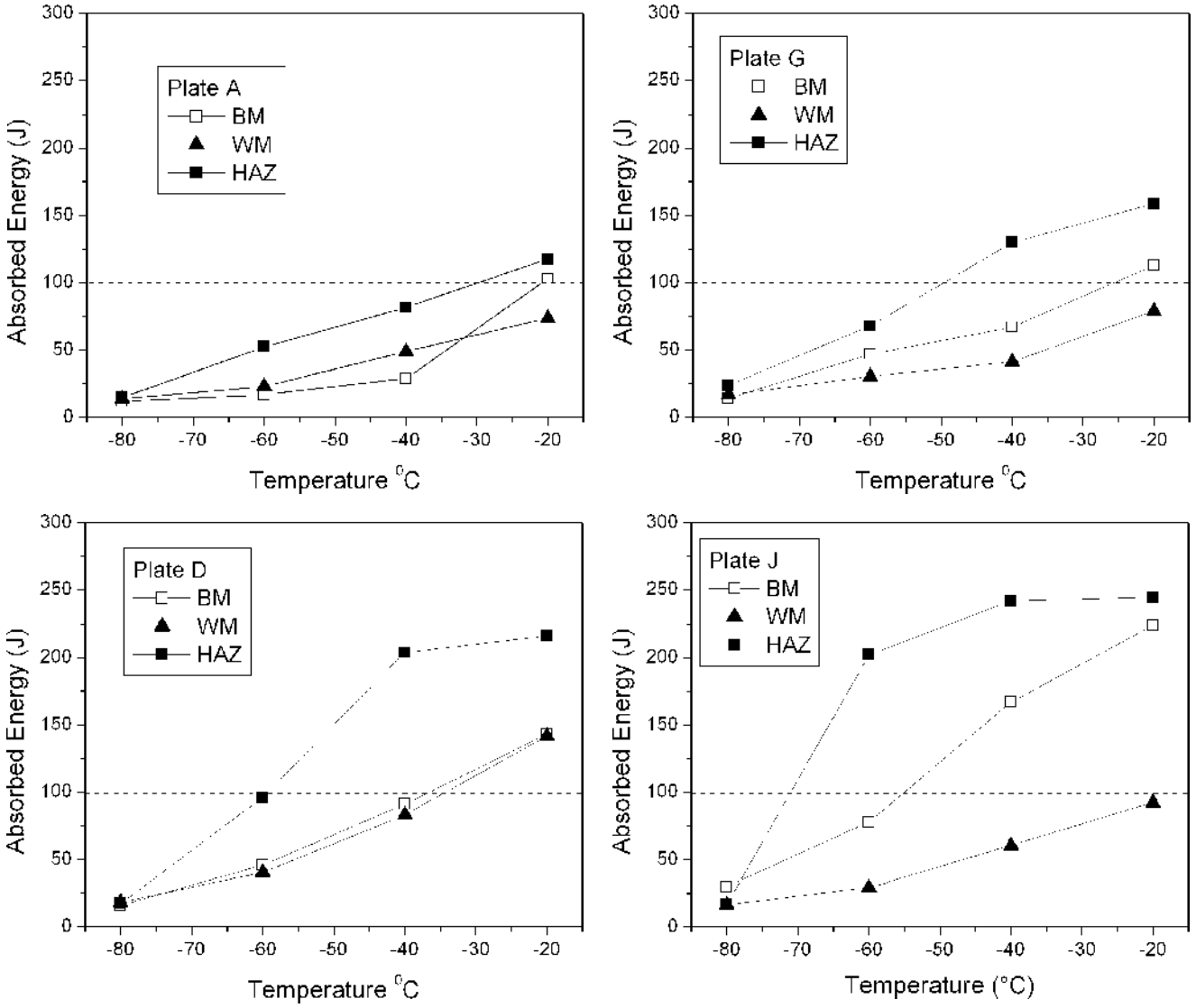

Fig. 7—Charpy-V absorbed impact energy curves.

The microstructural transformations imposed by the thermal cycles to the BM during longitudinal submerged arc welding did not affect the toughness of the HAZ. As shown in Figure 8, the HAZ showed high absorbed energy for all four tubes studied. In considering the three regions of the welded joint, BM, WM, and HAZ, the toughness results obtained for these alloys demonstrate that the HAZ was not the weak link. It should be observed that the HAZ toughness is compared with the body pipe as BM.

VII. RESISTANCE TO SCC AND HYDROGEN-INDUCED CRACKING

Both steels exhibited ductile behavior when subjected to the SSRT, testing in air, though the reduction in area (RA) measured for the X-70 (68 pct) was higher than that measured for the X-80 (60 pct). When tested in the thiosulfate solution described earlier (Table II), both steels exhibited a cleavage fracture morphology and the RA measurements maintained the tendency of the test in air, with the X-70 steel presenting a higher value, at 17 pct, than the X-80 (7 pct). The SCC susceptibility, as measured by the SSRT technique, is quoted as a relative ductility parameter. It can be seen that both steels were in fact found to be susceptible (Table V) as their relative ductility levels were low (<1).[22] A further indication of this tendency was the cleavage fracture mode exhibited by both steels, as previously mentioned.

No failure has been observed, after 720 hours, for the samples submitted to the traditional NACE test. Metallographic examination of longitudinal sections of samples exposed to both solutions, thiosulfate (Figure 8) and NACE (Figure 9), during the test revealed no indication of lateral surface or internal cracks. In this type of test, the fractographic analysis undertaken also showed no indication of secondary crack nucleation during the test.

VIII. DISCUSSION

The steel properties after controlled rolling were within the API standard specification. However, what makes the development of pipeline steel particularly difficult is that it is not enough to produce steels that attend the requirements of the API standard specification in the as-rolled state. It is also necessary to ensure that the steel will have good properties, including strength in aggressive environments, in the final tubular product, after the UOE process, both in the conformed plate and in the welded joint.

The main difference between the current pipeline steel and the existing pipeline steels is the production route. While this class of steels is usually produced by the process that involves accelerated cooling, the steel studied was produced using the traditional controlled rolling route. In order to do this, the rolling schedule and the composition had to be carefully optimized. To compensate for the absence of accelerated cooling, a higher content of alloying elements was necessary to provide a higher hardenability and a corresponding lower transformation temperature capable of generating a microstructure that would result in the desired mechanical properties.

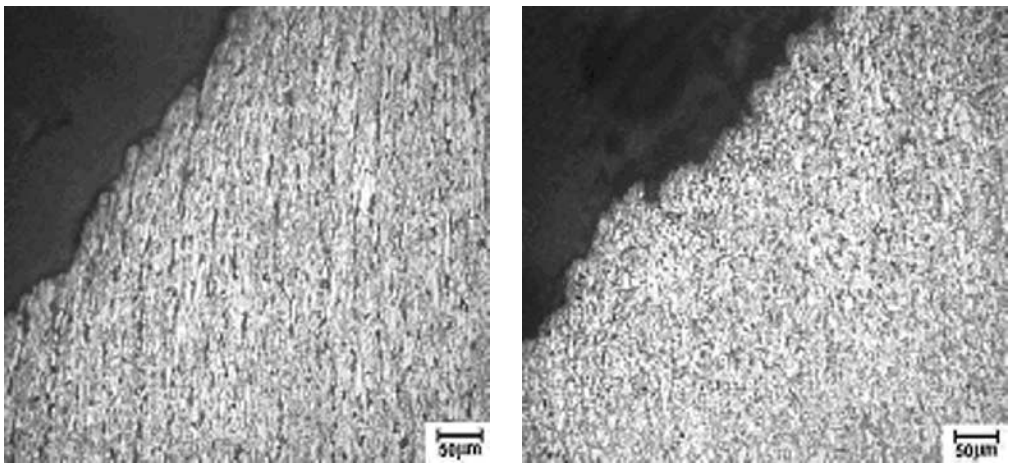

Table V. Results of the SSRT[17]

Test Piece		YS (MPa)	UTS (MPa)	RS* (MPa)	El* (Pct)	RA* (Pct)	Time to Rupture (s)	Susceptibility RA* (Pct)
X-70	air	450	610	408	23.1	68	38,220	0.25
	solution	460	611	522	—	17	27,120	
X-80	air	490	696	481	24.6	60	41,160	0.12
	solution	470	695	693	—	7	32,100	

Note: RS—rupture strength, El—elongation, and RA—reduction in area.

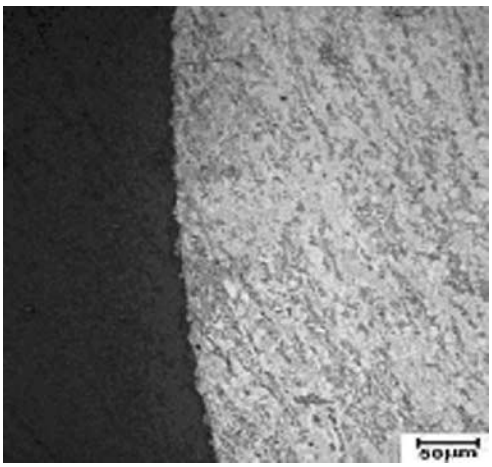

(*a*)

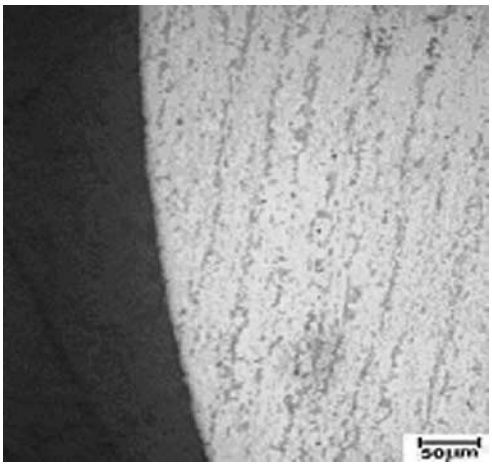

(*b*)

Fig. 9—Optical metallography of a section perpendicular to the NACE test piece surfaces for the X-70 and X-80 steels.[17]

The microstructure obtained was ferrite and contained the MA microconstituent (Figure 2) for both the NbCr and NbCrMo steel. In plate form, the steels under study presented an average absorbed energy of 200 J at −20 °C. In tube form, the same material, impact tested at the same temperature, exhibited average values of 150 J for the BM and 190 J for the HAZ. These results show that the steel properties meet the desired standards.

In the section that follows, each relevant aspect of the steel behavior, tensile properties after UOE processing, weldability, and resistance to SCC, is discussed with reference to the steel microstructure.

A. *Tensile Properties after UOE Processing*

It is well known that the mechanical properties of the steels at the plate stage of production are different from those of the final tubular product. For example, in considering the tensile strength aspects of the plate steel, one must account for the subsequent deformation from plate to tubular product, since the UOE process involves cold working. This cold working during the bending of the plate and the expanding of the tube will impose at least one stress reversal on the material.[23] It is important that after the UOE process, the tensile properties still meet the API X80 standard.

In general, pipeline steels can be classified into two categories according to their stress-strain behavior: Those that present a continuous stress-strain curve under tensile testing and those that present discontinuous stress-strain relationships. These differences in behavior can be explained in terms of the steel microstructure. Different steel microstructures will respond differently, for instance, ferritic-pearlitic steels tend to loose some strength after being UOE processed, while bainitic steels do not exhibit such a loss. Figure 3 shows the increase in strength of the alloys of this study through the YS/UTS relationship, after being subjected to the UOE process. Yet for both conditions, plate and tube, the YS/UTS relationship is below the maximum limit of 0.93 determined by the API 5L standard.

Therefore, the formability of these steels is adequate because their tensile properties after the UOE process comply with the API X-80 standard.

B. *Weldability*

The correct balance between strength and toughness can be lost in the HAZ owing to the thermal cycles and heat input levels typical of industrial welding processes. The pipeline steel must be able to maintain this balance, which is dependent on the chemical composition of the steel. As said previously, highly hardenable compositions had to be used here to compensate for the absence of accelerated cooling. This can have disadvantages with respect to weldability. This is mainly because a higher content of alloying elements results in a potentially higher CE, which should be in the range of 0.2 to 0.3 pct.[2] Usually, the HAZ has a lower toughness than the BM. Here, it was found that the HAZ had a slightly *higher* toughness than the BM. This is discussed in what follows with reference to the MA content of the microstructure. Moreover, the hardness and tensile properties of the HAZ are also relevant and are also discussed.

1. *HAZ toughness*

In the 1980s, the technical specifications for pipelines indirectly addressed the issue of weldability by the chemical composition limits imposed. According to the API 5L standard, the maximum carbon level for an X-65 steel was stipulated to be 0.26 pct, whereas for the X-70 grade, this maximum was lowered to 0.23 pct.[24] More modern high-strength low-alloy (HSLA) steels have been produced with a much lower C content of around 0.1 pct, and the tendency is to exploit even lower levels.

The current tendency to reduce the C level leads to a decrease in CE and reduces hardenability. For steels with C levels of around 0.1 pct, good weldability is achieved by the addition of appropriate alloying elements. The addition of Mn inhibits the formation of high-temperature transformation products such as pearlite and polygonal ferrite as well as promoting solid solution strengthening of the ferrite. Nickel, in addition to increasing hardenability, also increases toughness. Aluminum is exploited as a deoxidizing agent and, via nitride precipitation, as a grain refiner, whereas Nb serves to guarantee the precipitation processes, which retard austenite grain growth.[25]

The MA microconstituent volume fraction of the MA measured is related to the carbon content, in this study from

0.04 to 0.07 wt pct. The addition of microalloying elements also contributes to the formation of MA and thereby the weldability. Carbide forming elements such as Mo, Nb, and V retard the decomposition of MA. The addition of Mn, Cr, and Nb lowers the B_s temperature and promotes the formation of MA.[26]

In this study, it was observed that the volume fraction of MA increased with increasing CE (P_{cm}). For the same level of carbon, 0.04 pct, the NbCrMo steel exhibited a slightly lower P_{cm} than the NbCr steel. Naturally, the most significant increase in P_{cm} was caused by the increase in the level of carbon itself and, at a C level of 0.07 pct, the NbCrMo steel exhibited a P_{cm} of 0.18 pct.

In the published literature, it is mentioned that the presence of MA can be considered deleterious to toughness. It has also been observed, however,[6,12,27,28] that this deleterious effect is not only associated with MA volume fraction, but also with its morphology, size, and distribution in the matrix.

In the current study, the HAZ exhibited a higher MA volume fraction than the plate material (Table IV) as a result of the thermal cycling and heat input suffered during submerged arc longitudinal welding. Paradoxically, the toughness of the HAZ was found to be higher than that for the plate (Figure 8). This can be explained by reference to the differences in MA size and distribution, between the plate and the HAZ. As can be observed in Figures 2(c) and (d), the massive MA morphology was maintained for the HAZ of the NbCrMo and the NbCr steel, but the average particle size was observed to be smaller for the former, and the interparticle spacing was larger. Another factor that may have contributed to the increase in toughness of the HAZ was the fact that the MA particles are not interconnected. When the MA morphology is elongated and the microconstituents show an interconnected pattern, this results in low toughness. Therefore, the presence of MA can influence the toughness according to the MA morphology present in the microstructure. As seen previously (Figure 4), the increase in MA volume fraction for these alloys in the plate form resulted in an increase of ductile to brittle transition temperature (DBTT) when considering the 100 J absorbed impact energy level. However, when considering the same level of energy for the results obtained for the HAZ, a reduction in DBTT was observed (Figure 7). Since it is the same group of alloys and the only difference is the change of MA morphology during welding, as shown in Figures 2(a) and (c), all of the aforementioned MA-related factors, volume fraction, morphology, size, and distribution, may have contributed to the increase in the temperature associated with the 100 J absorbed impact energy level, as shown in Figure 7.

In summary, the HAZ, despite the relatively high heat input (~40 kJ/cm) and the high volume fraction of the MA microconstituent in the resulting microstructure, was shown to possess good toughness at low temperatures.

2. *HAZ hardness and tensile properties*

It is known that the thermal cycles associated with the industrial welding process used in pipeline fabrication and construction can lead to localized increases in hardness in the HAZ[21] and a reduction in the YS. No such increase was observed, however, for the steels and conditions studied in the current work (Figure 5). A similar result was presented by Dhua *et al.*[29] for a quenched and tempered HSLA100 steel of 14-mm thickness, with 0.04 pct C, 0.87 pct Mn, 0.25 pct Si, 0.5 pct Cr, 3.54 pct Ni, 0.57 Mo pct, and 0.038 pct Nb, after welding at a heat input of 2 kJ/mm.

It should be observed that, in the case of this study, the submerged arc process (Tandem technique), using three wires, produced a total heat input of approximately 40 kJ/cm. The reduction in hardness observed for the HAZ did not significantly affect the UTS values of the steel as compared with the plate and the welded joint, as shown in Figure 7(a). It was also observed, on tensile testing of the welded joints, that the rupture occurred in the BM away from the HAZ in all cases, as typified by the macrograph in Figure 6(b).

Usually, the design of a welded joint is defined in order to obtain a WM with similar or superior strength than the BM, never inferior. There was a difference in hardness, as indicated in the Figure 6(a); however, this difference is not enough to explain a variation in strength. Additionally, the relationship between hardness and strength is not linear for all microstructures.

Since the joint is constituted of three different regions, WM, HAZ, and BM, only the UTS of the welded joint is important. If the failure occurs in the WM, the material would not be approved since it was designed to have higher strength than the BM; if failure occurs at the HAZ, it is said to be embrittled. Therefore, the best result for a joint is when the failure occurs in the BM rather than the WM or HAZ

For the steels studied, for a given alloy, for example, NbCrMo type, varying the C content while maintaining the same composition with respect to the alloying elements, in order to produce P_{cm} values ranging from 0.18 pct (for 0.07 pct C) to 0.15 pct (for 0.04 pct C), resulted in no significant change in the HAZ hardness or the overall UTS of the welded joint.

C. *Resistance to SCC*

The capacity to design and produce pipeline steels with higher strength levels permits, from a mechanical properties standpoint, the use of thinner walled tubes for such applications. It must be remembered, however, that these materials are often exposed to aggressive service environments, and therefore, corrosion-related aspects will be a critical concern. With this in mind, the current study sought to compare the X-80 type steels under investigation here with a widely accepted X-70 pipeline grade of similar chemical composition.

The X-70 steel studied exhibited a ferrite-pearlite microstructure and the X-80 used for the comparison (plate G) had a ferrite with 3.4 pct MA volume fraction. It is important to note that the test pieces were prepared from samples taken from the body pipe.

Both steels exhibited ductile behavior when subjected to the SSRT in air, though the RA measured for the X-70 (68 pct) was higher than that measured for the X-80 (60 pct). When tested in the thiosulfate solution described earlier, both steels exhibited a cleavage fracture morphology, and the RA measurements maintained the tendency of the test in air, with the X-70 steel presenting a higher value, at 17 pct, than the X-80 (7 pct). The SCC susceptibility, as measured by the SSRT technique, is quoted as a relative ductility parameter. It can be seen that both steels were in fact found to be susceptible (Table VI), as their relative ductility levels were low (<1).[22] A further indication of this tendency was the cleavage fracture mode exhibited by both steels.

In general, the SCC process is composed of crack initiation and propagation, and the cracking of HSLA steels in the H_2S environment is dependent upon their hydrogen embrittlement susceptibility, where the evidence of H penetration is obtained from the presence of secondary microcracks and quasi-cleavage mode of fracture.[30]

Metallographic examination of longitudinal sections of samples exposed to both solutions, thiosulfate (Figure 8) and NACE (Figure 9), during the test revealed no indication of lateral surface or internal cracks. This is a good indication of the steel performance, considering that H is able to diffuse to sites with high triaxial tensile stress such as a crack tip, building up to a critical concentration, which can lead to hydrogen embrittlement.

A comparative analysis of the stress-strain curves is presented in Table V on the basis of the standard parameters: YS, UTS, RS, elongation at rupture (El pct), reduction in cross-sectional area at rupture (RA pct), and time to rupture. In the case of the tests conducted according to the NACE TM 0177/96—Method A (standard tensile test). Standard rupture did not occur for either of the steels investigated up to a test period of 720 h, even though the H_2S concentration in the solution used was several orders of magnitude higher than that in the thiosulfate solution used in the SSRT. A metallographic evaluation of the post-test specimen surfaces revealed no cracking, as shown in Figures 9(a) and (b).

The observed reduction in plasticity can be understood, in this case, as a reduction in the intrinsic toughness of the material, independent of the presence or absence of secondary cracks. The secondary cracking commonly associated with the internal hydrogen atom recombination mechanisms is promoted by the presence of nonmetallic inclusions. The observed loss of strength and plasticity was evident at high stress levels where a loss of toughness can be detected even for relatively low levels of hydrogen contamination. Similar results indicating high susceptibility were found for a X70 in the SSRT.[31]

Pipeline steels currently in service and widely studied are obtained by termo-mechanical controlled process (TMCP), which combines good toughness, high strength, and fine microstructure. Recent findings[30] showed that these microstructures play an important role in the crack initiation and propagation, and structures predominantly with acicular ferrite more suitable than ferritic-pearlitic microstructure for sour service.

The behavior of the two steels under study in the preceding tests in aggressive environments can be interpreted as indicating good resistance to those hydrogen-induced damage mechanisms associated with the internal recombination of hydrogen atoms introduced into the material as a result of corrosion-related reactions, since no secondary cracks were found in either test. However, since there was a reduction in ductility for both steels in the SSRT, the microstructural characteristics evidently result in some susceptibility to SCC, as mentioned previously. It must be stressed that the SSRT is useful for laboratory evaluations of hydrogen-associated damage mechanisms, but that the dynamic nature of the applied loading and stressing into the plastic regime imposed in this type of testing are not typical of service conditions. In this respect, the static, elastic regime, NACE test is undoubtedly a better indicator of steel behavior in service-like conditions.

In summary, the loss in ductility for both X-70 and X-80 steels tested, detected during the SSRT in sodium thiosulfate solution, indicates some susceptibility to SCC. This type of test, however, does involve hydrogen contamination during plastic deformation, which is not a condition likely to occur in pipeline service. The NACE test, under conditions of nonplastic loading, showed the two steels to exhibit a good performance in this respect, with no evidence being detected of a loss in strength for the imposed conditions. In neither test were secondary cracks observed.

IX. CONCLUSIONS

The production an of API class steels using the traditional controlled rolling route with careful adjustment of steel composition demonstrated that it is possible to use a hardenable steel to achieve ferrite/bainite in two, NbCr and NbCrMo, steel systems. The microstructure obtained was correlated not only with the resulting mechanical properties, but also with the weldability and strength in aggressive environments to which the materials are exposed. This shows that it is possible to obtain steel of this class without accelerated cooling attending the requirements of the API 5L standard specification.

ACKNOWLEDGMENTS

The authors acknowledge the financial support of FINEP and PETROBRAS and the technical support of USIMINAS, CONFAB, and CENPES-PETROBRAS for this study. The authors are also grateful to CNPq and FAPERJ for their financial support and Professor J. Ponciano (PEMM/COPPE/UFRJ, Brazil) for the use of laboratory facilities and technical assistance in performing the SSRTs.

REFERENCES

1. J.M. Gray and W.J. Fazakerley: *37th Annual Conf. of Metallurgists*, Calgary, AB, Canada, 1998, August 16–19, CIM, Canada, 1998, pp. 1-31.
2. C. Ouchi: *Iron Steel Inst. Jpn. Int*., 2001, vol. 41 (6), pp. 542-53.
3. M. Nagae, S. Endo, N. Mifune, N. Uchitomi, and O. Hirano: *NKK Rev*., 1992, vol. 66, pp. 17-24.
4. K. Hulka: *Niobium Information*, CBMM/NPC, 1997, No. 13/97, pp. 1-42.
5. I. Hrivnak, F. Matsuda, and K. Ikeuchi: *Trans. JWRI*, 1992, vol. 21, pp. 9-32.
6. Y. Li, D.N Crowther, M.J.W. Green, P.S. Mitchell, and T.N. Baker: *Iron Steel Inst. Jpn. Int*., 2001, vol. 41 (1), pp. 46-55.
7. P.R. Rios and R.W.K. Honeycombe: *Mater. Sci. Technol*., 1990, vol. 6, pp. 838-84.
8. P.A. Manohar and T. Chandra: *Iron Steel Inst. Jpn. Int*., 1998, vol. 38, pp. 766-74.
9. D.P. Fairchild: *Proc. Int. Symp. on Welding Metallurgy of Structural Steels*, TMS, Warrendale, PA, 1987, pp. 303-18.
10. C. Thaulow, A.J. Paauw, and K. Guttormsen: *Welding J*., 1987, vol. 59, pp. 266s-279s.
11. D.P. Fairchild, N.V. Bangaru, J.Y. Koo, P.L. Harrison, and A. Ozekcin: *Welding J*., 1991, vol. 70, pp. 321s-329s.
12. C.L. Davis and J.E. King: *Mater. Sci. Technol*., 1993, vol. 9, pp. 8-15.
13. P.S.A. Bezerra: Master's Thesis, Catholic University of Rio de Janeiro, Rio de Janeiro, 1998 (in Portuguese).
14. NACE International: NACE Standard TM0177/96, Standard Test Method, NACE, Houston, TX, revised Dec. 1996.
15. G.Z. Batista, L.F.G. de Souza, Ivani de S. Bott, and P.R. Rios: *Proc. Int. Conf. on Thermomechanical Processing: Mechanics, Microstructure & Control*, E.J. Palmiere, M. Mahfouf, and C. Pina, eds., University of Sheffield, Sheffield, England, 2003, pp. 240-44.

16. *Specification for Line Pipe*, API Specification 5L, American Petroleum Institute, Washington, DC, 2000.
17. K.R.S. Lima: Master's Thesis, University of Rio de Janeiro, Rio de Janeiro, 2002 (in Portuguese).
18. Ivani de S. Bott: *Int. Conf. on Processing and Manufacturing of Advanced Materials THERMEC '2003*, T. Chandra, J.M. Torralba, and T. Sakai, eds., part 2, Trans. Tech. Publications Ltd., Switzerland, 2003, vols. 426–432, pp. 1463-68.
19. F.B. Pickering: *Physical Metallurgy and the Design of Steels*, Materials Science Series, Applied Science Publishers, London, 1978, pp. 60-88.
20. Y. Ito and K. Bessyo: *J. Jpn. Welding Soc*., 1968, vol. 37 (9), pp. 983-91
21. B. Dixon and K. Hakansson: *Welding J*., 1995, vol. 74, pp. 122s-132s.
22. A.L.L.T. Small: Master's Thesis, Federal University of Rio de Janeiro, Rio de Janeiro, 1996 (in Portuguese).
23. A.M. Sage: *Proc. Conf. Steels for Line Pipe and Pipeline Fittings*, The Metals Society, 1981, pp. 39-50.
24. B.L. Jones: *ASM Int. Conf. on Technology and Applications of HSLA Steels*, Philadelphia, PA, 1983, *ASM*, Metals Park, OH, 1984, pp. 715-22.
25. T.W. Montemarano, B.P. Sack, J.P. Gudas, M.G. Vassilaros, and H.H. Vanderveldt: *J. Ship Production*, 1986, vol. 2, pp. 145-62.
26. F. Matsuda, Y. Fukada, H. Okada, C. Shiga, K. Ikeuchi, Y. Horii, T. Shiwaka, and S. Suzuki: *Welding World*, 1996, vol. 37, pp. 134-54.
27. F. Kawabata, M. Okatsu, K. Amano, and Y. Nakano: *Pipeline Technol*., 1995, vol. 2, pp. 263-71.
28. H. Ikawa, H. Oshige, and T. Tanoue: IIW DOC IX-1156-80, International Institute of Welding, London, 1980.
29. S.K. Dhua, D. Mukerjee, and D.S. Sarma: *Iron Steel Inst. Jpn. Int*., 2002, vol. 42, pp. 290-98 and 42-50.
30. M.C. Zhao, B. Tang, Y.Y. Shan, and K. Yang: *Metall. Mater. Trans. A*, 2003, vol. 34A, pp. 1089-96.
31. A. Albiter, A. Contreras, M. Salazar, and R. Perez: *Proc. 7th Int. Congr. of Pipelines*, Puebla, Mexico, 2003.